Biophysical Journal, Volume 97

Supporting Material

A RasGTP-Induced Conformational Change in C-RAF Is Essential for Accurate Molecular Recognition

Kayo Hibino, Tatsuo Shibata, Toshio Yanagida, and Yasushi Sako

SUPPORTING MATERIALS

Single-molecule kinetics of Ras-RAF interactions

The on-time distributions ($f(t)$) of GFP–RAF from RasGDP, and GFP–RBD from RasGDP or RasGTP can be described by simple stochastic dissociation kinetics (S1):

$$f(t) \propto \exp(-kt) \qquad (1)$$

Here, k is the dissociation rate constant. Fitting the on-time distributions with this function returned best-fit values of k = 3.7, 3.5, and 2.9 s^{-1} for GFP–RAF from RasGDP, GFP–RBD from RasGDP, and GFP–RBD from RasGTP, respectively (Fig. 2, C, E and F in the text). These results suggest that the association states in these three cases are similar and involve interactions between the RBD of RAF and RasGDP or RasGTP. The dissociation rate of RBD from RasGTP is similar to that from RasGDP. This may explain why GFP–RBD cannot fully distinguish RasGDP from RasGTP (Fig. 2, E and F in the text).

The on-time distributions of GFP–RAF from RasGTP and RBDCRD–GFP from RasGDP or RasGTP suggest a kinetic intermediate in the dissociation process (Fig. 2, D, G and H in the text). As the simplest case, the following reaction scheme is assumed:

$$\mathrm{M1} \xrightarrow{k_1} \phi$$

$$\mathrm{M1} \xrightarrow{k_2} \mathrm{M2} \xrightarrow{k_3} \phi$$

Here, M1 and M2 are the initial association state and the kinetic intermediate of the Ras-RAF (or Ras-RBDCRD) interaction on the plasma membrane, respectively. ϕ is the dissociation state. k_1, k_2, and k_3 are the rate constants for the dissociation from the initial state, for the formation of the kinetic intermediate, and for the dissociation from the kinetic intermediate, respectively. According to this reaction scheme, the on-time distribution can be described by the following function:

$$f(t) \propto \frac{1}{p-q}\left\{p(k_1-q)e^{-pt} - q(k_1-p)e^{-qt}\right\} \qquad (2)$$

Here, $p+q = k_1 + k_2 + k_3$ and $pq = k_1k_3 + k_2k_3$.

Fitting the on-time distribution for GFP–RAF from RasGTP, and RBDCRD–GFP from RasGDP or RasGTP with equation (2) returned best fit values of $k_1 < 10^{-14}$, indicating that the direct dissociation from the initial association state, M1, was negligible. The best-fit values for k_2 and k_3 can be obtained from equation (2) or from $f(t) \propto t\exp(-pt)$ when $p \approx q$. These values of k_2 and k_3 are 2.4 and 0.82 s^{-1} for GFP–RAF from RasGTP; 1.9 and 1.9 s^{-1} for RBDCRD–GFP from RasGDP; and 1.9 and 1.9 s^{-1} for RBDCRD–GFP from RasGTP (k_2 and k_3 are

interchangeable because k_1 is negligible).

REFERENCE

S1. Xie, S. 2001. Single-molecule approach to enzymology. *Single Molecules* 2:229-236.

SUPPORTING FIGURES

Figure S1 | Dual-view optics for imaging single-pair FRET in living cells. (**A**) Block diagram of the hand-made dual-view optics used in this study to image the single-pair FRET from GFP to YFP in live cells. BPX/Y: band-pass filter with the center of transmission at X nm and a full band width of Y nm. DMX: dichroic mirror transmitting wavelengths longer than X nm. L: lens. LPX: long-pass filter with cut-off wavelength of X nm. M: mirror. (**B**) Single-molecule images of GFP (upper) and YFP (lower) acquired using the dual-view optics. The leakage of the GFP signal to the YFP (525–540 nm) channel and the YFP signal to the GFP (500–525 nm) channel was 86% and 35%, respectively. Scale bar: 5 μm.

Figure S2 | Changes in the single-molecule fluorescence intensity from the FRET probe. (**A**) Typical single-molecule traces of the fluorescence intensity from the GFP–RAF (wild type)–YFP probe in quiescent cells (left) and cells 1–5 min after stimulation with EGF (right) are shown. The fluorescence intensities observed in the GFP (black) and YFP (red) channels are plotted against the time after association with Ras. Lines with the same symbols (circles, triangles, or squares) indicate the same molecules. Fluorescence intensities in the GFP channel increased after stimulation with EGF, suggesting a reduction in FRET efficiency. Intensities in the YFP channel also increased after stimulation with EGF, with leakage of GFP fluorescence. (**B**) The unmixed GFP (black) and YFP (red) fluorescence were calculated for each fluorescent spot in (**A**) using the single-molecule fluorescence of GFP and YFP as references. YFP intensities decreased after stimulation with EGF (right).

Figure S3 | Accumulation of RAF and fragments of RAF at the plasma membrane. Confocal images of live HeLa cells expressing GFP–RAF, GFP–RBD, or RBDCRD–GFP were acquired (Fig. 1 in the text). The relative fluorescence intensity in the peripheral regions of the cells was measured against the total intensity in the cells as an indication of the accumulation of each molecule at the plasma membrane. Average values for the relative intensities after subtraction of the average relative intensity of GFP alone (Fig. 1D in the text) are plotted with their standard deviations. For each measurement, 8–18 cells were examined. The accumulation of RBD at the plasma membrane was low, even after the cells were stimulated with EGF. RBDCRD accumulated at the plasma membrane independently of EGF stimulation.

Figure S4 | Distributions of RAF molecules in cells expressing RasV12 and RasN17. (**A**), HeLa cells transiently coexpressing GFP–RAF and RasV12 (constitutively active mutant of Ras) were observed by scanning confocal microscopy. The cells were not stimulated with EGF. GFP–RAF accumulated at the plasma membrane. This result indicates that the activation of Ras is sufficient to induce the translocation of RAF to the plasma membrane and supports the prevailing concept that RasGTP is the initial association site of GFP–RAF at the plasma membrane of cells stimulated with EGF (Fig. 1A in the text). (**B**), Cells transiently coexpressing RBDCRD–GFP and RasN17 (dominant negative mutant of Ras) were observed. The cells were not stimulated with EGF. RBDCRD–GFP accumulated at the plasma membrane. RasN17 depletes RasGTP by competing with RasGDP for the guanine nucleotide exchange factor. RasN17 itself is a nucleotide-free form of Ras. Therefore, this result suggests that the accumulation of RBDCRD at the plasma membranes of quiescent cells (Fig. 1C in the text) is not caused by its association with the minor population of RasGTP molecules in quiescent cells, thereby supporting the concept that RBDCRD associates firmly with the inactive forms of Ras (RasGDP and/or RasN17). Scale bar: 10 μm.

Figure S5 | Single-molecule detection of GFP-tagged RAF. (**A**), Typical time course of fluorescence intensity changes in GFP–RAF at the plasma membrane of fixed (left) and live (right) HeLa cells. For fixation, the cells were treated with –20 °C methanol for 2 min. Step-like photobleaching is shown at the left and suggests the detection of single molecules. Lines in different colors represent results from different molecules. (**B**), Fluorescence intensity distributions of GFP–RAF spots observed on the plasma membrane of fixed (left) and live (right) HeLa cells. Lines represent fitting with the two-component Gaussian distribution. Arrows show the peaks and percentage fractions of the fitting. N represents the number of spots examined. The intensities of the first peaks are similar to the photobleaching step sizes shown in (**A**), suggesting that most of the GFP–RAF spots observed in the live cells are single molecules.

Figure S6 | Single-molecule imaging of the association between GFP–RAF and RasGDP. (**A**–**C**) HeLa cells coexpressing GFP–RAF and DsRed–Ras were prepared. Fluorescence images of GFP–RAF (**A**) and DsRed–Ras (**B**) were obtained in the same field of view using epifluorescence microscopy. Single molecules of GFP–RAF were observed in the same fields using total internal reflection fluorescence (TIRF) microscopy (**C**). Outlines of the cells are shown as dashed lines. The cells were not stimulated with EGF. Scale bar: 10 μm. (**D**) On-time

distribution of GFP–RAF in cells overexpressing Ras. In cells overexpressing DsRed–Ras (**B**), the numbers of single molecules of GFP–RAF increased (**C**), even though the expression levels of GFP–RAF were similar in all cells (**A**). However, the on-time distribution of GFP–RAF in cells overexpressing Ras was similar to that of the RBD fragment or GFP–RAF in cells without exogenous Ras expression (Fig. 2 in the text). These results suggest a specific association between RasGDP and RAF.

Figure S7 | On-time distributions of GFP–RAF–YFP. Single molecules of GFP–RAF–YFP expressed in HeLa cells were observed using a TIRF microscope, and their on-time distributions were examined before (left) and after (right) stimulation with EGF to induce Ras activation. The distributions are similar to those for GFP–RAF in cells before and after stimulation with EGF (Fig. 2, C and D in the text). N indicates the number of GFP–RAF–YFP spots observed under each condition. The lines show the results of fitting the distribution with the functions described in Supporting Materials. The best fit values are $k = 1.7\ s^{-1}$ for the left distribution and $k_1 < 10^{-14}$ and $k_2 = k_3 = 1.7\ s^{-1}$ for the right distribution. These rate constants differ slightly from those of GFP–RAF, probably because of the conjugation of YFP to the C terminus, but the interaction of GFP–RAF–YFP with RasGDP or RasGTP can be described using the same kinetic functions as those for GFP–RAF.

SUPPORTING MOVIES

Movie S1 | Single-molecule imaging of GFP–RAF in a quiescent cell. Single molecules of GFP–RAF observed in a HeLa cell. The movie is in real time with a frame rate of 30 s^{-1}. Image size is 36 × 36 μm.

Movie S2 | Single-molecule imaging of GFP–RAF in a cell stimulated with EGF to induce Ras activation. Single molecules of GFP–RAF observed in a HeLa cell after stimulation with EGF. The movie is in real time with a frame rate of 30 s^{-1}. Image size is 36 × 36 μm.

Movie S3 | Intramolecular single-pair FRET imaging of GFP–RAF–YFP in a quiescent cell. Single molecules of GFP–RAF–YFP observed in a HeLa cell. Signals were separated into the GFP (left) and YFP (right) channels using dual-view optics before the camera. A cell is present on the right side of the dashed lines. The movie is in real time with a frame rate of 30 s^{-1}. Image size is 48 × 20 μm.

Movie S4 | Intramolecular single-pair FRET imaging of GFP–RAF–YFP in a cell stimulated with EGF to induce Ras activation. Single molecules of GFP–RAF–YFP observed in a HeLa cell after stimulation with EGF. Signals were separated into the GFP (left) and YFP (right) channels using dual-view optics before the camera. A cell is present on the right side of the dashed lines. The movie is in real time with a frame rate of 30 s^{-1}. Image size is 48 × 20 μm.

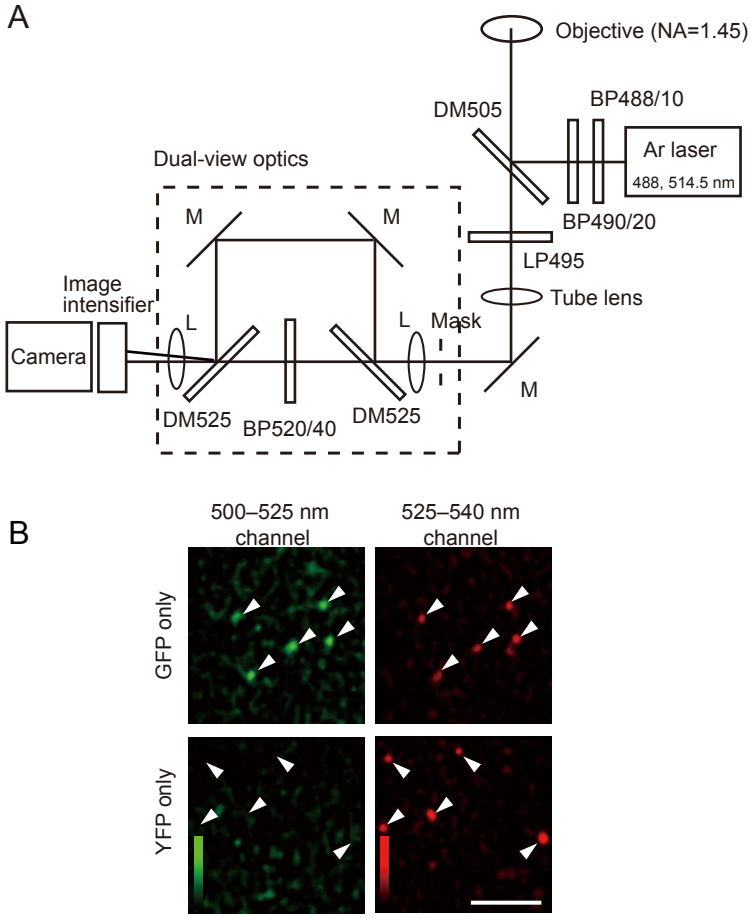

Figure S1. Hibino *et al.*

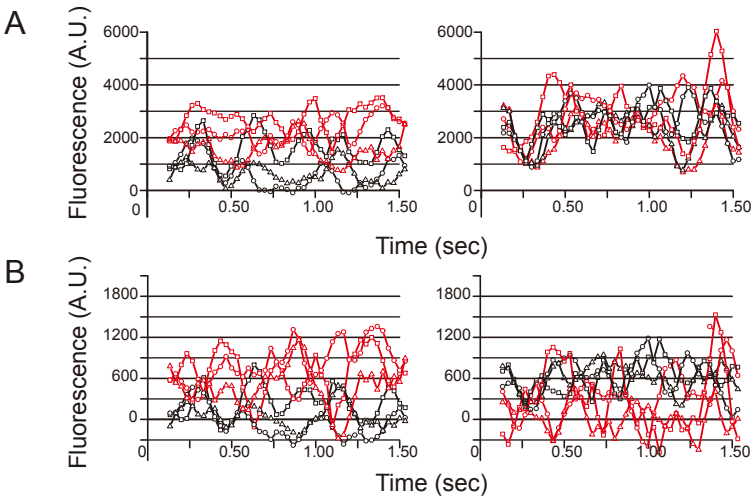

Figure S2. Hibino *et al.*

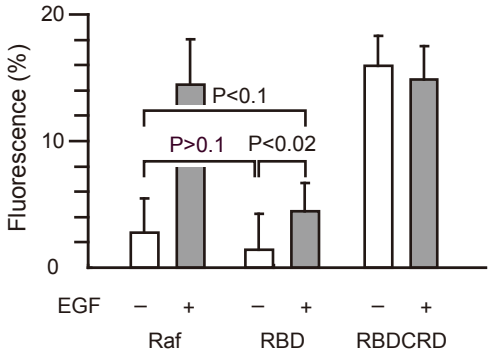

Figure S3. Hibino *et al.*

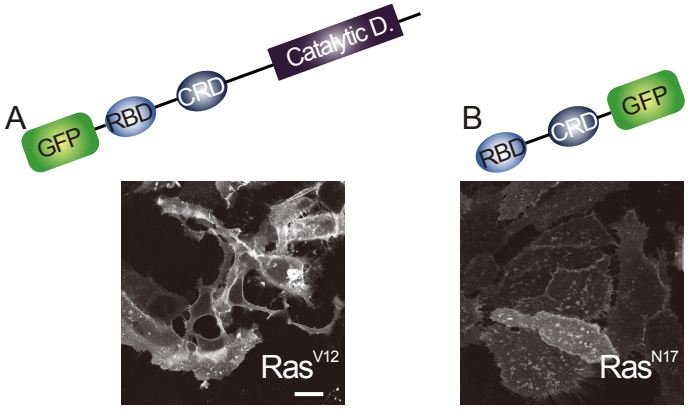

Figure S4. Hibino *et al.*

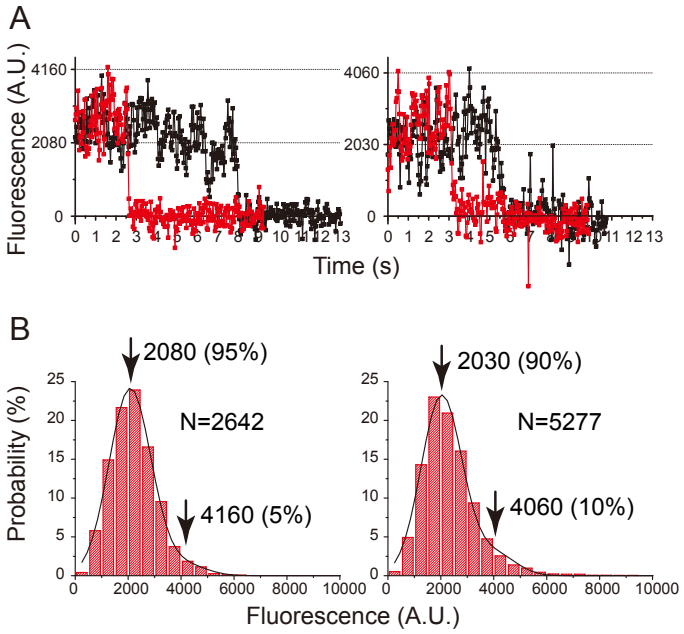

Figure S5. Hibino *et al.*

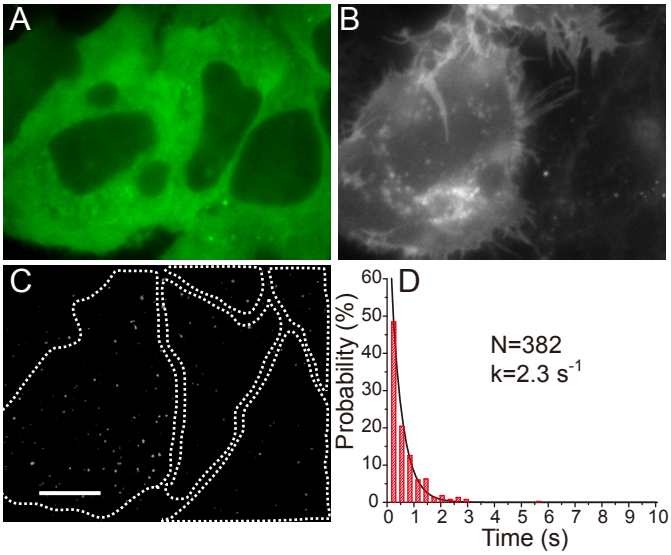

Figure S6. Hibino *et al.*

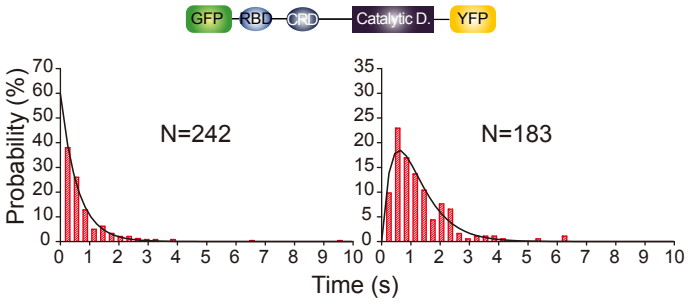

Figure S7. Hibino *et al.*